Plasmon Energy Analysis of Hydride Phases in Zr-2.5wt%Nb CANDU Pressure Tubes

Sang-Yeob Lim[a]*, Soon-Hyeok Jeon, Hee-Sang Shim
Materials Safety Technology Research Division, Korea Atomic Energy Research Institute, Republic of Korea
E-mail: sylim@kaeri.re.kr

***Keywords : Pressure tube Hydride, Scanning transmission electron microscopy, Electron energy loss spectroscopy**

1. Introduction

Zirconium alloys are used in reactors due to their small neutron absorption cross-section and excellent corrosion resistance. In the case of Canada Deuterium Uranium (CANDU) reactors, the Zr-2.5Nb alloy is used as the material for pressure tubes [1-3]. However, in zirconium alloys, hydrogen adsorption is inevitable due to contact with water, which is used as a coolant or neutron moderator during reactor operation [4-7]. The long-term ingress of hydrogen leads to the formation of hydrides in this alloy during hydrogen charging. The generation of hydrides significantly degrades the integrity of the material through mechanisms such as delayed hydride cracking, which is important when considering the long-term safety of the reactor.

Therefore, the behavior of hydrogen within the pressure tubes of CANDU reactors has garnered interest in academia, and there are generally two types of hydrides observed in terms of low hydrogen concentration in the Zr-H system. These are the face-centered cubic (FCC) δ-hydride with a stoichiometry between $ZrH_{1.5}$ (Zr_2H_3) and $ZrH_{1.67}$ (Zr_3H_5), and the face-centered tetragonal (FCT) γ-hydride ZrH, which represents hydrogen atoms aligned within the lattice. The δ-hydride is perhaps the most commonly observed and is typically formed during slow cooling [8–12]. In contrast, the formation of γ-hydride is often associated with rapid cooling in zirconium alloys containing low concentrations of hydrogen [13–16].

However, there is still a lack of clear understanding regarding the phenomena of hydrides, even at the boundaries of δ-hydride formation. This paper aims to apply a hydride analysis method utilizing EELS plasmon and to develop a code for imaging, thereby presenting a new method for visually assessing the newly developed hydrides. Additionally, this study evaluates the phase analysis of hydrides and the formation of hydrides at the phase boundaries of δ-hydride.

2. Experimental

2.1 Hydrogen Charging in Zr-2.5Nb

In this experiment, the Zr-2.5Nb alloy was used as the material for pressure tubes, and its chemical composition is shown in Table 1. To form hydrides, hydrogen was charged onto the material surface using an electrolytic method. Initially, 1 mol of sulfuric acid was used as the electrolyte for hydrogen charging at a temperature of 85±5°C. Subsequently, a current of 100 mA/cm² was applied for 24 hours to achieve hydride formation on the material surface. Additionally, vacuum tubing (using Pyrex) was performed to diffuse hydrogen into the pressure tube material. Afterward, the material was homogenized at 350 °C for 240 hours, during which no microstructural changes were observed. The material was then slowly cooled from the Pyrex vacuum tube.

Table I: Chemical composition of Zr-2.5Nb (wt.%).

Element	Zr	Nb	Fe	O	N	P
wt.%	97.4	2.5	0.05	0.097	0.007	0.003

2.2 Analysis of Hydrogen Concentration and Hydride Formation in Homogenized Samples

After performing surface hydride charging, heat treatment was conducted to homogenize the hydrogen concentration within the material. After that, a cube sample with dimensions of 3 mm^3 was produced, and the hydrogen concentration of the material was measured using a hydrogen analyzer (LECO RH-404, LECO Corporation, USA). The hydrogen concentration was measured three times, and the average value was taken. To confirm the distribution of hydrides, a surface etchant consisting of a mixture of distilled water, nitric acid, and hydrofluoric acid was used, with a molar ratio of 4:4:2 for etching, and the material was analyzed using an optical microscope.

2.3 Hydride Analysis Using TEM and EELS

To analyze the hydrides using transmission electron microscopy (TEM), the material was electrochemically polished using a mixture of 90% methanol and 10% perchloric acid. Initially, 25 V was applied to a jet polishing system (TenuPol-5) for electro-polishing. Additionally, the hydrides were analyzed using the high-angle annular dark field (HAADF) STEM imaging capability of an atomic resolution analytical electron microscope (JEM-ARM200F, JEOL Ltd., Tokyo, Japan). Plasmon energy loss was analyzed using an EELS system (GIF Quantum® LS imaging filter, Gatan, Inc., CA, USA). Furthermore, the analyzed data were imaged according to plasmon energy using in-house developed code.

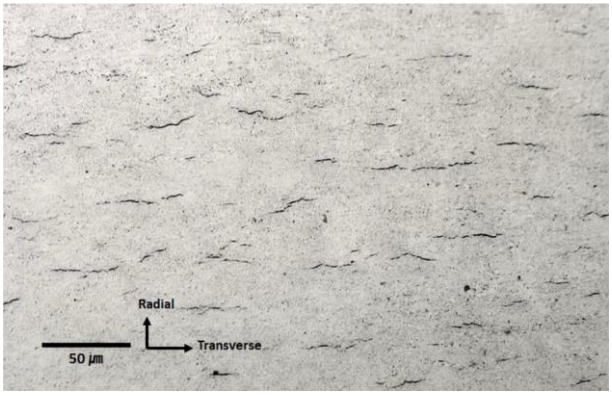

Fig. 1. Micrograph of the hydrogen-charged Zr-2.5 wt.% Nb alloy, with a hydrogen concentration of 86 wppm.

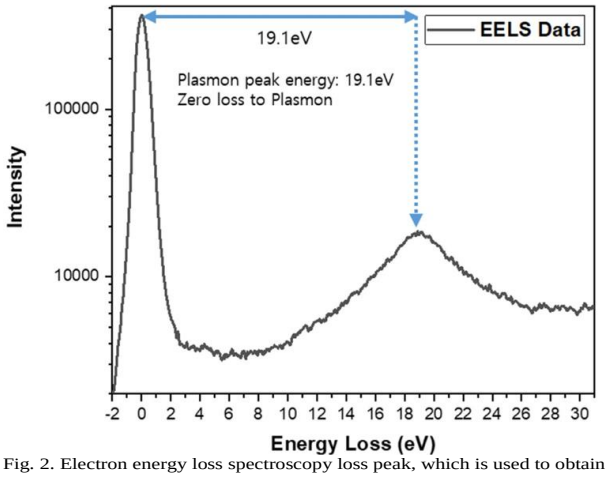

Fig. 2. Electron energy loss spectroscopy loss peak, which is used to obtain the plasmon peak value

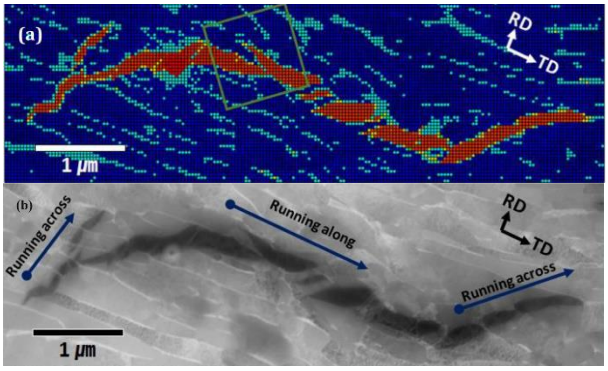

Fig. 3. Microstructural image and diffraction analysis using high-angle annular dark-field (HAADF) scanning transmission electron microscopy.

3. Results and discussion

3.1. Analysis of Hydrides Using Optical Microscopy

The amount of hydrogen within the material was evaluated at 86 wppm using a hydrogen analyzer. Additionally, this hydrogen is shown to exist in the form of hydrides, as illustrated in Figure 1. The average length of the hydrides is approximately 50 μm, and the hydrides are oriented parallel to the transverse direction.

3.2. Characterization of Hydride Phases Using EELS

After visualizing the EELS analysis data as a 2D image, the 2D plasmon energy loss is presented in Figure 3(a). The plasmon energy loss was measured, applying the previously known energy ranges, and the plasmon peak energies for α-Zr, γ-hydrides, and δ-hydrides are known to be 16.8-16.9 eV, 18-18.3 eV, and 18.8-19.2 eV, respectively. Therefore, considering a certain margin on both sides, the plasmon peak energies corresponding to each phase are indicated in blue, yellow, and red. Additionally, the region of 17.3-17.8 eV, which could not be represented in the data, is shown in cyan. Subsequently, by overlaying the data with the HADDF image, it was confirmed that the cyan image corresponds to β-Zr.

4. Conclusion and future works

In this study, we utilized EELS equipment to measure plasmon energy and presented the results in a 2D image. Based on this 2D image and HADDF image, we analyzed α-Zr and δ-hydrides, revealing an energy range of 17.3-17.8 eV that remains undefined, which corresponds to β-Zr. Additionally, we confirmed the existence of a γ-hydrides region between α-Zr and δ-hydrides; however, further in-depth discussions are necessary for a clearer definition of this region. Future research will focus on additional experimental and theoretical analyses of the properties and mechanisms of γ-hydrides to deepen our understanding of this area and explore the potential applications of related materials.

ACKNOWLEDGEMENTS

This work was supported by the National Research Foundation (NRF) grant funded by the Korean government (Grant No. RS-2022-00143316)

REFERENCES

[1] S.S. Kim, S. Lim, D.H. Ahn, G.G. Lee, K. Chang, Effect of Inhomogeneous Nucle- ation of Hydride at α/β Phase Boundary on Microstructure Evolution of Zr–2.5 wt% Nb Pressure Tube, Met. Mater. Int. 25 (4) (2019) 838–845.
[2] L.B. Golden, I.R. Lane, W.L. Acherman, Corrosion resistance of titanium, zirconium, and stainless steel, Ind. Eng. Chem. 44 (1952) 1930–1939.
[3] B. Lustman, F. Kerze, The Metallurgy of Zirconium, vol. 4, McGraw-Hill Book Company, London, 1955.
[4] Nuclear Fuel, Cladding, and the "Discovery" of Zirconium, in: T. Filburn, S. Bullard (Eds.), Three Mile Island, Chernobyl and Fukushima, Springer, Cham, 2016, pp. 105–114.
[5] R.N. Singh, N. Kumar, R. Kishore, S. Roychaudhury, T.K. Sinha, B.P. Kashyap, De- layed hydride cracking in Zr–2.5 Nb pressure tube material, J. Nucl. Mater. 304 (2-3) (2002) 189–203.
[6] S-Q. Shi, G.K. Shek, M.P. Puls, Hydrogen concentration limit and critical tem- peratures for delayed hydride cracking in zirconium alloys, J. Nucl. Mater. 218 (2) (1995) 189–201.

[7] S. Sagat, C.K. Chow, M.P. Puls, C.E. Coleman, Delayed hydride cracking in zirco- nium alloys in a temperature gradient, J. Nucl. Mater. 279 (1) (2000) 107–117.
[8] E. Zuzek, J. P. Abriata, A. San-Martin, F.D. Manchester, The H-Zr (hydrogen-zirconium) system, Bull. Alloy Phase Diagrams. 11 (1990) 385–395.
[9] C. P. Kempter, R. O. Elliott, K. A. Gschneidner, Thermal expansion of delta and epsilon zirconium hydrides, J. Chem. Phys. 33 (1960) 837–840.
[10] E. A. Gulbransen, K. F. Andrew, Crystal Structure and Thermodynamic Studies on the Zirconium-Hydrogen Alloys, J. Electrochem. Soc. 101 (1954) 474.
[11] D. O. Northwood, Gamma and delta hydrides in zirconium alloys, J. Less-Common Met. 48 (1976) 173–175.
[12] K. E. Moore, W. A. Young, Phase studies of the Zr-H system at high hydrogen concentrations, J. Nucl. Mater. 27 (1968) 316–324.
[13] J. S. Bradbrook, G. W. Lorimer, N. Ridley, The precipitation of zirconium hydride in zirconium and zircaloy-2, J. Nucl. Mater. 42 (1972) 142–160.
[14] I. Ferguson, J. E. Bailey, The Analysis of Hydrides in Hydrogen-Zirconium Alloys Cooled from the-Zirconium Phase Field, J. Appl. Crystallogr. 6 (1973) 351–354.
[15] E. Tulk, M. Kerr, M. R. Daymond, Study on the effects of matrix yield strength on hydride phase stability in Zircaloy-2 and Zr 2.5wt% Nb, J. Nucl. Mater. 425 (2012) 93–104.
[16] J. E. Bailey, Electron microscope observations on the precipitation of zirconium hydride in zirconium, Acta Metall. 11 (1963) 267–280.